

Fabrication of Micro Spiral Phase Plates in Fused Silica using F₂-Laser Microstructuring

Sebastian Buettner, Michael Pfeifer and Steffen Weissmantel
Laserinstitut Hochschule Mittweida, Technikumplatz 17, Mittweida, Germany

Keywords: Fluorine Laser, Fused Silica, Microstructuring, Orbital Angular Momentum, Spiral Phase Plates.

Abstract: The results of our investigations on direct laser fabrication of micro spiral phase plates (SPPs) in fused silica using the fluorine laser microstructuring technique will be presented. The process, which based on the mask projection technique, enables the generation of SPPs with different topological charges, handedness, modulation depths and level numbers. For this, a special double mask rotation system was developed, which allows the fabrication of micro SPPs with an individual configuration with regard to the mentioned parameters. Moreover, the phase of a spherical lens can be added to the helical phase of the SPP using a special mask geometry. Furthermore, we build up a measurement system for a first optical characterization of the fabricated SPPs.

1 INTRODUCTION

Nowadays data communication become more important, than ever. But the capacity of optical channels is limited by nonlinear effects in fibers, using classical wavelength or polarization multiplexing (Richardson, 2010). Regarding to the expected increase of the data traffic and the desired transmission speed, new multiplexing methods are required. One of these new method is to use the orbital angular momentum (OAM) of light, which could enhance the capacity of optical data communication channels (Xie et al., 2018). Moreover, the integration of electro-optical systems become more interesting and has been realized also the field of data communication (Neitz et al., 2017). For this purpose, we developed a new method for the fabrication of Fresnel lenses using the fluorine laser microstructuring technique (Pfeifer et al., 2015). In the last few years, a variety of methods and techniques were developed to manufacture optical elements in the micrometer scale and in particular for polymer and other low melting materials (Kasztelanic et al., 2013; Xing et al., 2016; Qui et al. 2018). Whereas the available fabrication techniques for the processing of fused silica and other wide band gap materials are limited. The fluorine laser microstructuring technique provides a very flexible alternative to lithographic processes. Based on our research in microstructuring of blaze gratings (Pfeifer, Weissmantel and Reisse, 2013), diffractive optical elements

(Pfeifer et al., 2014), cylindrical lenses and lens arrays (Buettner, Pfeifer and Weissmantel, 2019), we now developed a method for the fabrication of micro spiral phase plates. This could be interesting for a new kind of integrated optical multiplexing systems, which based on the OAM of light.

2 FUNDAMENTALS AND EXPERIMENTAL SETUP

2.1 Orbital Angular Momentum

The wavelength, amplitude, phase and polarization are well known properties of electromagnetic waves (EMW). The latter is also known as the spin angular momentum of photons. But there is another kind of momentum, the OAM, which was measured first by Allen et al., in 1992 (Allen et al., 1992). This momentum results from helical phase which is characterized by an azimuthal phase term. The modulation of an even wave front with a helical phase term gives the linear momentum of the photons an azimuthal component. The summation of this components enhance the OAM. Due to this, this momentum is a result of the interaction of several photons (Allen and Padgett, 2011). Nevertheless, this can be used to encode classical information. There are some methods to create light and in particular laser beams with a defined

OAM. One of them is to use a vortex grating, the other is to use an SPP. Both methods were already used for data communication experiments (Xie et al., 2018; Bozinovic et al. 2013).

2.2 Calculation of the Process Parameters for SPP Fabrication

Using SPPs is an effective and flexible way to generate very different and individual OAMs. SPPs are a special kind of diffractive phase elements and in general assigned to the group of computer generated holograms. These elements can be used to convert a Gaussian intensity distribution to a circular intensity distribution. This can be reached by modulating the phase of an even EMW with a helical phase shift. In general the efficiency of diffractive phase elements depends on the number of levels (O’Shea et al., 2004). For our investigations we have chosen three different numbers of levels (8, 16, 32). Regarding to the design wavelength and the appropriate optical thickness of the material for a 2π phase shift, the step size has to be calculated. A phase shift of 2π is equal to a modulation depth of $m = \pm 1$. The sign of the modulation depth defines handedness of the helical phase. A right-handed SPP lead to left-handed OAM of a transmitting EMW from the backside.

For our investigations, we have chosen the common laser wavelength of 532 nm. For this, the refractive index ($n = 1.46$) of the fused silica Corning 7980 were calculated using the Sellmeier equation. The corresponding depth of the microstructure at a modulation depth of 2π is 776.72 nm. The required ablation depth per pulse and the appropriate laser pulse fluence for different numbers of levels was calculated using the Lambert-Beer’s law and the appropriate ablation parameters of the material (see Table 1).

Table 1: Calculated step size and required laser pulse fluence (ablation threshold and absorption coefficient for Corning 7980: $H_{th} = 0.56 \text{ J/cm}^2$, $\alpha = 12.98 \cdot 10^4 \text{ cm}^{-1}$).

level	step size	laser pulse fluence
8	97.09 nm	1.97 J/cm ²
16	48.42 nm	1.05 J/cm ²
32	24.27 nm	0.77 J/cm ²

2.3 Microstructuring Process

The microstructuring is done by the laser micromachining station EX-157, which was built by 3D-Micromac AG. A detailed description of the station is given in our previous work. The setup is basically

comparable to the one for the fabrication of micro Fresnel-lenses.

The microstructuring process is based on the mask projection technique. By using a pulsed excimer laser system, every laser pulse remove a certain amount of material depending on the laser and material parameters. Due to the homogenization of the laser beam, the laser pulse fluence H is homogenously distributed in the whole mask area and thereby in the image plane of the imaging system too. Therefore, the ablation depth is the same in the whole ablation area. This area is formed by the mask geometry. In general, the depth of the microstructures depends on the laser pulse fluence and the number of pulses per area. The generation of a helical phase shift can be done by influencing the optical thickness of a transparent material. For this, the required structure is comparable to a spiral staircase. The fabrication of these three dimensional microstructures requires the control of the microstructuring depth within the ablation area and in particular in rotation direction. This can be realized by a combination of two semi-circular masks, which are placed in a row. A sample is shown in Figure 1. For this, a mask rotation system was developed. This system consists of two rotary axis. Both masks can be rotated independently by separate drives. The system is shown in Figure 1.

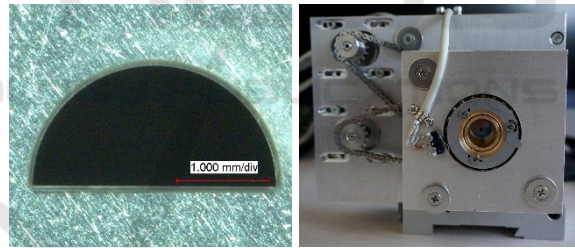


Figure 1 and Figure 2: Semi-circular mask in tantalum-foil for the fabrication of SPPs with a diameter of 100 μm (l.) and developed double rotation system with two servo drives for independent and separate movement of the masks (r.).

The micro structuring process starts with the calculation of the sector angle and the step angle from the topological charge (TC), which represents the number of 2π phase jumps within the structure. Furthermore, the number of levels N_i defines the step angle of the target structure. The masks are in congruent position after the referencing of the system. Following, one of the masks is twisted toward the other until the sector angle is reached. This position is the initial state for the microstructuring of each sector, independently from the sector angle. In consideration of the TC, the orientation of the resulting mask changes

for each sector. Starting from this initial state, the sector angle is reduced by the step angle after every laser pulse. This process is repeated until the number of required steps is reached. In this way the SPPs were fabricated sector by sector. The process is realized in a sequence of loops and can be influenced by the TC, the level number and the laser pulse fluence. The latter defines the ablation depth per pulse, which defines the vertical step size. One advantage of these technique is, that we are able to fabricate irregular SPPs. However, a disadvantage is, that the topological charge has to be at least two and the process is limited by the resolution of the imaging system in general and accuracy of the mechanic components as well. After the fabrication, we removed the remained debris by etching the sample 30 min in a 1.7 molar KOH solution, followed by 15 min ultrasonic cleaning.

3 RESULTS AND DISCUSSION

3.1 Geometrical Properties of the Fabricated SPPs

The fabrication of SPPs in fused silica with different TCs is possible by changing the number of sectors N_l and the corresponding sector angle. For regular SPPs the sector angle is an integer fractional part of 360 degree. A set of fabricated SPPs with different TCs and level numbers are shown in Figure 3. As can be seen in this Figure, the sectors of the SPPs in the upper row are well fabricated.

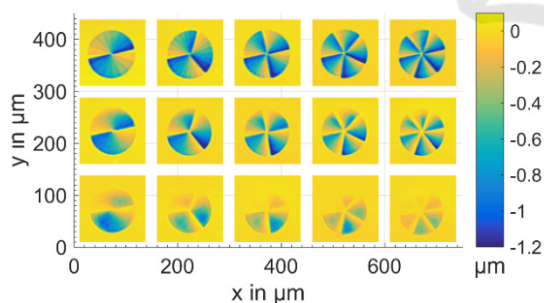


Figure 3: Three dimensional micrographs (top view) of fabricated SPPs in Corning 7980 with $m = 1$, a TC of 2, 3, 4, 5 and 6 (left to right) and a level number of 8, 16 and 32 (top to bottom).

This is caused by the higher laser pulse fluence and the appropriate ablation depth per pulse. The SPPs in the middle and lower row got an uneven depth within the sectors. The Reason for this is the inhomogeneity of the energy distribution of the laser beam. The used laser system is currently not in tune.

Because of a low damage threshold of some optical components, the homogenizer is de-adjusted. Due to this, the energy distribution of the laser beam is slightly in-homogenous. The fabrication of SPPs with a higher level number requires a lower step size and thereby a lower laser pulse fluence. The fabrication of SPPs with 32 levels requires an ablation depth per pulse of 24.27 nm. Due to this, the used laser pulse fluence is $H = 0.77 \text{ J/cm}^2$, which is just a little more than the ablation threshold fluence of $H_{th} = 0.56 \text{ J/cm}^2$ of the material. Because of this, the error of the ablation depth within the ablation area increase and summed up by the number of pulses. In this way, the inhomogeneity of the laser beam is transferred to the surface and in particular to the microstructure. Nevertheless, it is possible to fabricate left-handed SPPs (see Figure 4).

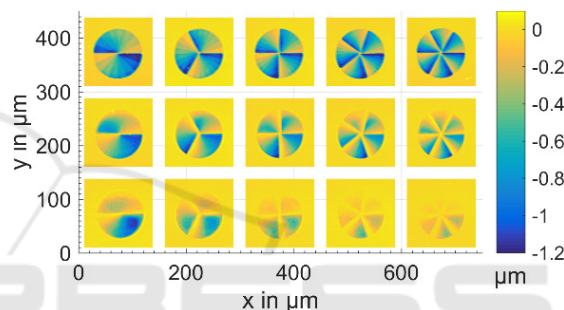


Figure 4: Three dimensional micrographs (top view) of fabricated SPPs in Corning 7980 with $m = -1$, a TC of 2, 3, 4, 5 and 6 (left to right) and a level number of 8, 16 and 32 (top to bottom).

In this case, the calculations and starting conditions are the same. However, the motion of the axis were interchanged and the feed direction is inverted. As a result, the microstructuring depth increase in the counter clockwise direction, as can be seen. In Figure 5 the circular profile sections of the 8-level SPPs are shown. The radius of the circular section was set to $R_s = 25 \mu\text{m}$. As can be seen, the single slope within one SPP is nearly equal. In general the microstructuring depth is in the range of 900 nm which is slightly more than the required 776.72 nm. Furthermore, the last step is significantly deeper than the previous steps.

The reason for this is the accumulation of radiation, which is reflected at the steep edge of the structure. Moreover, the lateral step size become smaller by increasing the TC. An increase of this lead to a reduction of the sector angle as well as the step angle and the corresponding lateral step size. Furthermore, it can be seen that the arc length of the sectors are not equal. The reason for this, is possibly a malfunction

of the rotation system. This problem can maybe solved by some constructive changes. The comparison of one sector of an 8-, 16- and 32-level SPPs with a topological charge of 2 shows the influence of the level number and the required reduction of the vertical step size (see Figure 6).

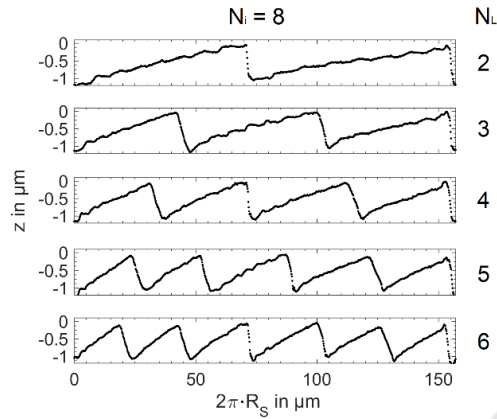


Figure 5: Circular profile section of the 8 level SPPs with different TCs.

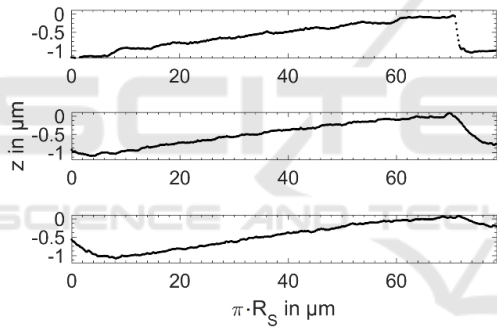


Figure 6: Circular profile section of one sector of an 8-, 16- and 32-level SPP with a TC of 2.

The increase of the numbers of levels once more lead to the reduction of the lateral step size. Due to this the profile section of the 32-level SPP is more continuous than the section of the 8- and 16-level SPPs. In consideration of the radial dependencies of this, it is not possible to fabricate a complete continuous surface with this technique. Furthermore, it can be seen that the steep edge of the structure also become flattened by increasing the number of levels. Thereby the gained efficiency is affected by geometrical inaccuracies. One option to avoid these, is to increase the modulation depth. The SPPs, which are shown in Figure 7, were fabricated with a laser pulse fluence of 1.97 J/cm^2 .

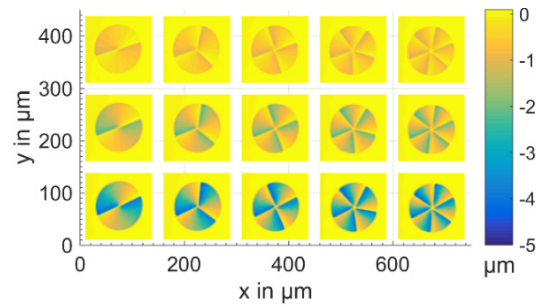


Figure 7: Three dimensional micrographs (top view) of fabricated SPPs in Corning 7980 with a m of -1, -2 and -4, a TC of 2, 3, 4, 5 and 6 (left to right), a level number of 8, 16 and 32 (top to bottom) and constant vertical step size.

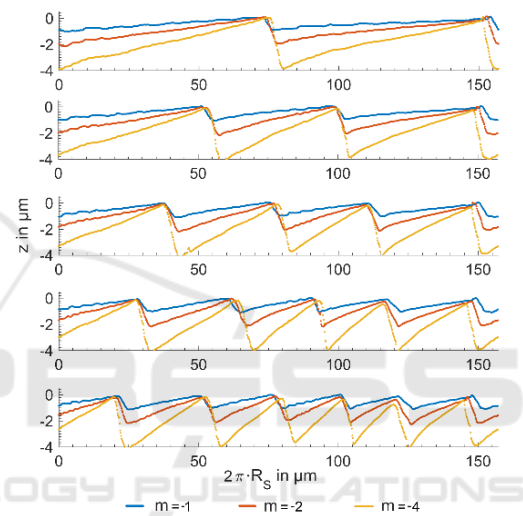


Figure 8: Circular profile section of the 8, 16 and 32 level SPPs with a modulation depths m of -1, -2 and -4.

To increase the modulation depth, the number of levels were increased only. The SPPs which were shown in Figure 7 are left handed, with an m of -1 (upper row), -2 (middle row) and -4 (lower row). The increase of the OAM by increasing the level number, lead to a surface profile with a more continuous course, as can be seen in Figure 8.

3.2 SPPs with Lens Term

To show further opportunities of this fabrication technique, we calculated some different kinds of masks. One calculated mask pair is shown in Figure 9. Regarding to this, the left mask is the semi-static mask, which defines a constant sector angle. Because of the asymmetric geometry of the rotation mask (right), it is not possible to influence the sector angle like using the semi-circular masks. At the beginning of the process the masks have to be in congruent position with

regard to their rotation center and lower edges. This kind of masks enables the fabrication of SPPs with an additional radius of curvature (ROC) and straight sector edges, as can be seen in Figure 10.

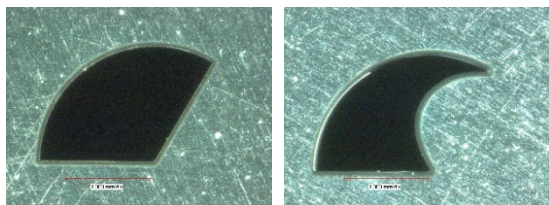


Figure 9: Semi-static mask (left) and rotary mask (right) for SPP fabrication with additional radius of curvature (ROC).

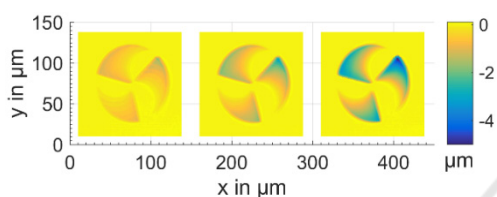


Figure 10: Three dimensional micrographs (top view) of three fabricated SPPs in Corning 7980 with an m of -1, -2 and -4, a TC of 3 and a level number of 8, 16 and 32 (left to right).

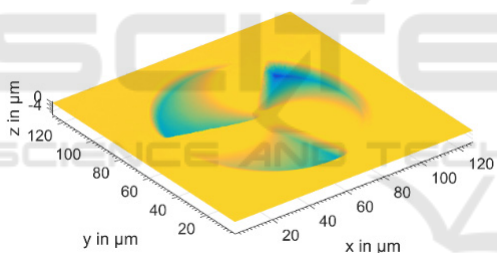


Figure 11: Three dimensional micrograph of a SPP with additional ROC.

But this combination got also a big disadvantage. It is not possible to get the whole sector structured, as can be seen in Figure 11. To solve this problem, the micro structuring process has to be divided in two processes.

In a first sequence one sector of the SPP has to be fabricated like described in the previous chapter. In a second sequence, the fabricated staircase structure has to be structured again, using the corresponding mask geometry for lens fabrication. The calculation method for this and the parameter dependencies were subject of previous investigations. For this setup, there are different ways to solve this problem. The first is to reduce the sector angle of the semi-static mask to the half of the rotation mask. The second is to enlarge the mask aperture angle of the rotation mask to the twice angle of the semi-static mask. One

of these configurations allows the described procedure. This can lead to a microstructuring process where the level number, the OAM and the ROC can be influenced independently. Only the TC is given by the mask itself. The third method is to calculate two nearly identical masks with curved radial edges of the sector. But the one mask has to be reversed to the other because they are placed in opposite of each other. Due to the curved edges of the mask, the edges of the sectors of the SPPs become also curved. The advantages of this configuration are the same like the semi-circular masks. But the ROC is not independently adjustable with regard to the level number, the handedness and also the vertical step size. However, we calculated two semi-circular masks with defined curved sector edges, as can be seen in Figure 12.

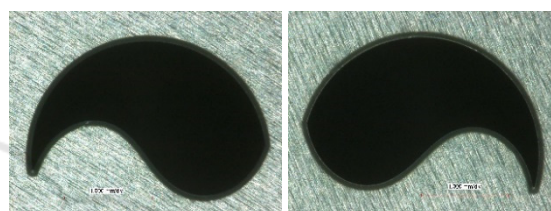


Figure 12: Set of semi-circular masks with curved edges.

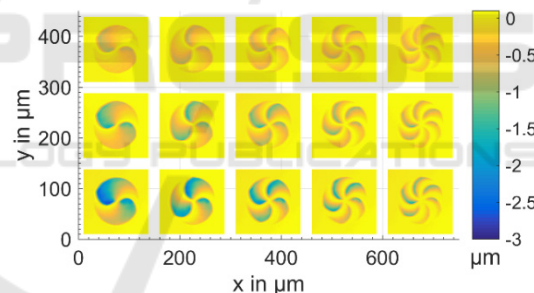


Figure 13: Three dimensional micrographs (top view) of SPPs with an m of -1, -2 and -4 (top to bottom), an additional ROC, curved sector edges and different level numbers (8, 16 and 32 from top to bottom).

And as intended, using these masks lead to curved sector edges. This is shown in Figure 13. The calculated ROCs of the structures are in the range of 1 to 16 mm, depending on the TC and the level number. But we are currently not able to measure the ROC of these structures. For this we need to develop a special evaluation algorithm which separates the spherical from the helical structural percentage. This should be done in consideration of some well selected and defined boundary conditions, which we did not defined yet. Furthermore, we have to take some fabrication defects into account, which we cannot separate from the structure easily.

3.3 Testing the Optical Function

To prove the optical function of these elements, we set up a simple measurement system, where the sample is illuminated by a frequency doubled Nd:YAG laser. The intensity of the laser beam can be adjusted by two polarizers (P). For the detection of the radiation, we used a confocal microscope. A schematic illustration of the measurement setup is shown in Figure 14. With this we are able to measure the relative intensity distribution of a set of SPPs in a defined plane behind the sample. Because of some geometrical limitations, we can capture the diffraction image in a maximum distance of 3 mm.

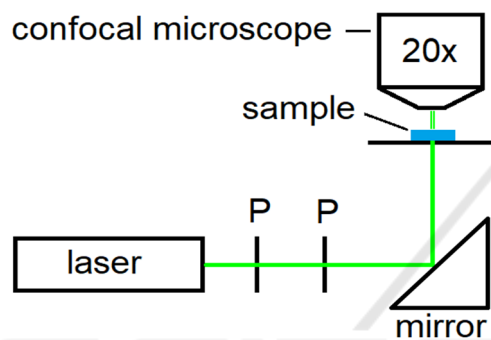


Figure 14: Illustration of the measurement setup.

As can be seen in Figure 15 and Figure 16 the number of intensity maxima increase with the number of TCs. The distributions which are generated by SPPs in the lower rows, are very different. This is caused by the fabrication errors, which were discussed in chapter 3.1. Moreover, there are some smaller intensity maxima in the center of the shown distributions in the upper and the middle row. The reason for this is the unstructured area in the center of the SPPs. This is mainly a result of the limited resolution of the imaging system of the micro machining station in combination with adjusting and imaging errors. Furthermore, it can be seen that the intensity distributions of the SPPs with the same configuration but different handedness is the inverted of each other.

However, with this measurement setup it is not possible to see a significant influence of the level number. Furthermore, there are interfering effects between adjacent distributions. To prevent this, the spot of the laser beam has to be reduced. If this is not sufficient a pinhole could be placed on axis to the SPP. The relation of the pinhole and beam diameter should be selected in a right way, to avoid any diffraction effects. In comparison to the level number, the influence of the modulation depth can be seen clearly. The diffraction image in Figure 17 is generated by the

SPPs which are shown in Figure 7. The increase of the modulation depth lead to a circular formation of the intensity maxima. Moreover, the maxima are laterally reduced in radial direction. The diffraction images in the lower row show also a subdivision of the ring distribution. The reason for this could be the interaction of the lateral step size (and corresponding level number) and the TC. In this case, the higher level number could lead to a very small lateral step size. These steps may act as a circular phase grating, in superposition with the helical phase.

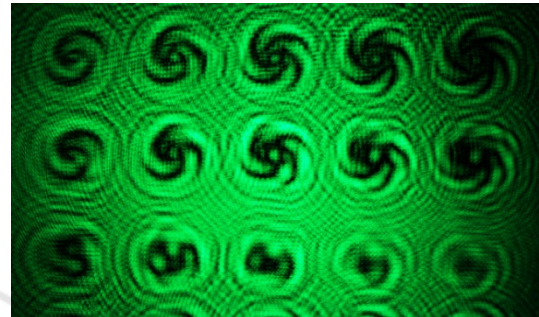


Figure 15: Confocal microscope image of the intensity distribution 3 mm above the SPPs are shown in Figure 3 (OAM⁻).



Figure 16: Confocal microscope image of the intensity distribution 3 mm above the SPPs are shown in Figure 4 (OAM⁺).

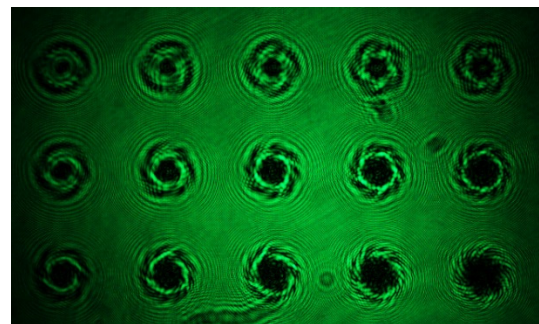


Figure 17: Confocal microscope image of the intensity distribution 0.49 mm above the SPPs with different modulation depth.

In addition, the SPPs which were fabricated with the curved semi-circular masks were also optically examined. As can be seen in Figure 18, the curved steps and sectors lead to a further reduction of the maxima size in rotation direction.

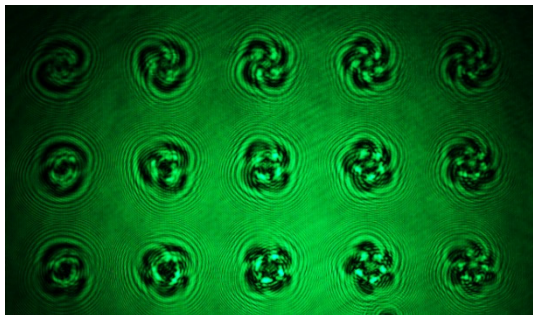


Figure 18: Intensity distribution of transmitting radiation through SPPs 0.49 mm above, with different modulation depth and additional ROC (SPPs shown in Figure 13).

As a result, the optical response of the SPPs includes a defined number of intensity maxima depending on the TC. The ROC decrease by the increase of the TC and the level number. This could lead to a reduction of the maxima size and thereby an increase of the intensity too. Like in the previous investigations, the influence of the level number is not apparent. This could be solved by upgrading the measurement system for single SPP characterization with optimized measurement conditions.

4 CONCLUSIONS

The fabrication of SPPs with different TCs, level numbers, handedness and modulation depths is possible using the fluorine laser microstructuring technique. For this, a double mask rotation system was developed and installed.

The fabrication of simple SPPs can be done using two semi-circular masks. Furthermore, these allows the fabrication of SPPs with different configurations by changing the process and programming parameters. This enables the fabrication of SPPs with a TC of 2 to 6. The number of intensity maxima within the optical response of the SPPs is equal to the TC. In general, the fabrication of SPPs with an irregular TC is possible. Due to some little inaccuracies in the arc length of the sectors, the rotation system should be optimized.

An increase of the level number lead to a more continuous surface profile and enhance the efficiency of the SPPs but requires a very low laser pulse fluence

for a 2π modulation depth. As a result, the slightly inhomogeneous energy distribution of the laser beam is transferred into the microstructure. This affect the optical function of the SPPs. To solve this problem the modulation depth can be increased. But this also got an influence on the OAM and lead to the reduction of the size of the intensity maxima in radial direction.

In addition to this, the SPPs can be fabricated including a ROC in two different ways. The first is to calculate a set of masks for the fabrication of a defined SPP. The other way is to calculate two semi-circular masks with curved edges. Using the latter lead to a more flexible process in comparison to the first. But for this the ROC cannot be influenced independently from the other parameters. However, an additional ROC lead to a further reduction of the size of the intensity maxima. The influence of the step size should be the subject of further investigations and supported by some theoretical studies. For the improvement of the optical characterization, the measurement system should be improved too.

Moreover, we want to build up an optical link using some lenses first, followed by using a fiber as a transfer medium. Depending on the results, further investigations will be done in the field of OAM multiplexing using integrated optics.

ACKNOWLEDGEMENTS

The authors gratefully acknowledge the financial support of the present work by the European Union and the Free State of Saxony.



Europäische Union

Europa fördert Sachsen.



Europäischer Sozialfonds



Diese Maßnahme wird mitfinanziert durch Steuermittel auf der Grundlage des vom Sächsischen Landtag beschlossenen Haushaltes.

REFERENCES

- Allen, L., Beijersbergen, M.W., Spreeuw, R.J.C. and Woerdman, J.P. (1992). Orbital angular momentum of light and the transformation of Laguerre-Gaussian laser modes. In *Physical Review A*, 45(11), pp. 8185-8189.
- Allan, L. and Padgett, M. (2011). The Orbital Angular Momentum of Light: An Introduction, In: *Twisted Photons*, eds. Torres J.P and Torner L., pp. 1-12.

- Bozinovic, N., Yue, Y., Ren, Y., Tur, M., Kristensen, P., Huang, H., Willner, A.E. and Ramachandran, S. (2013). Terrabit-Scale Orbital Angular Momentum Mode Division Multiplexing in Fibers. In *Science*, 340 (6140), pp. 1545-1548.
- Buettner, S., Pfeifer, M., and Weissmantel, S. (2019). Manufacturing of Cylindrical Micro Lenses and Micro Lens Arrays in Fused Silica and Borosilicate Glass using F₂-Laser Microstructuring. *7th International Conference on Photonics, Optics and Laser Technology*.
- Kasztelaniec, R., Kujawa, I., Stępień, R., Haraśny, K., Pysz, D. and Buczyński, R. (2013). Molding of soft glass refraction mini lens with hot embossing process for broadband infrared transmission systems. In *Infrared Physics & Technology*, 61, pp. 299-305.
- Neitz, M., Wöhrmann, M., Zhang, R., Fikry, M., Marx, S. and Schröder, H. (2017). Design and Demonstration of a Photonic Integrated Glass Interposer for Mid-Board-Optical Engines, *67th Electronic Components and Technology Conference*.
- O'Shea, D.C., Suleski, Th.J., Kathman, A.D. and Prather, D.W. (2004). *Diffraction Optics. Design, Fabrication, and Test*. Bellingham, Washington USA: SPIE, pp. .
- Pfeifer, M., Büettner, S., Zhang, R., Serbay, M. and Weißmantel, S. (2015). F₂-Lasermikrostrukturierung von Mikro-Fresnel-Linsen, In *Journal of the University of Applied Sciences Mittweida*, pp. 127-130.
- Pfeifer, M., Jahn, F., Kratsch, A., Steiger, B. and Weissmantel, S. 2014. F₂-Laser Microfabrication of Diffractive Optical Elements, *2nd International Conference on Photonics, Optics and Laser Technology*.
- Pfeifer, M., Weissmantel, S. and Reisse, G. 2013. Direct laser fabrication of blaze gratings in fused silica. In *Applied Physics A* 112, pp. 61-64.
- Qiu, J., Li, M., Ye, H., Yang, C., and Shi, C. (2018). Fabrication of high fill factor cylindrical microlens array with isolated thermal reflow. In *Applied Optics*, 57(25), pp. 7296-7302.
- Richardson, D. J. (2010). Filling the Light Pipe. In *Science*, 330 (6002), pp. 327-328.
- Xie, Z., Gao, S., Lei, T., Feng, S., Zhang, Y., Li, F. Zhang, J., Li, Z. and Yuan, X. (2018). Integrated (de)multiplexer for orbital angular momentum fiber communication. In *Photonics Research*, 6 (7), pp. 743-749.
- Xing, J., Rong, W., Sun, D., Wang, L. and Sun, L. (2016). Extrusion printing for fabrication of spherical and cylindrical microlens arrays. In *Applied optics*, 55 (25), pp. 6947-6952.